

AD-A040 316 CARNEGIE-MELLON UNIV PITTSBURGH PA DEPT OF METALLURG--ETC F/6 11/6
ALUMINIDE COATING OF IRON.(U)
MAY 77 R W HECKEL, C OUCHI, M YAMADA
UNCLASSIFIED TR-2

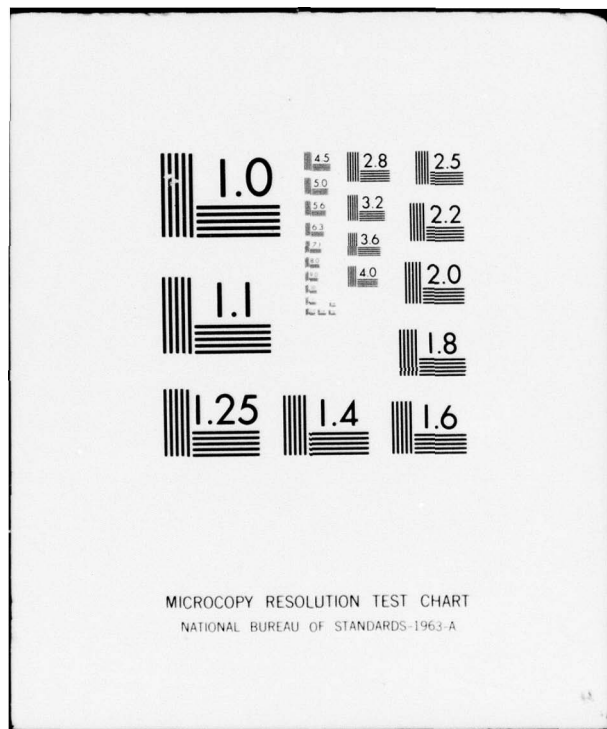
N00014-76-C-0198

NL

| OF |
AD
A040316
EE

END

DATE
FILMED
7-77



ADA 040316

AD No. DDC FILE COPY

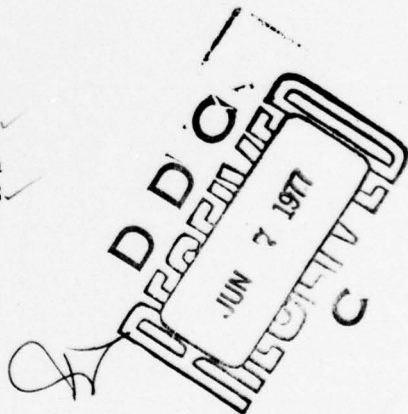
(12)
B.S.

ALUMINIDE COATING OF IRON

R. W. Heckel, M. Yamada, C. Ouchi and A. J. Hickl

Technical Report No. 2
Office of Naval Research
Contract N00014-76-C-0198

May 1977



Reproduction in whole or in part is permitted for
any purpose of the United States Government.

Distribution of this document is unlimited.

Carnegie-Mellon University
Department of Metallurgy and Materials Science
Pittsburgh, Pennsylvania 15213

Aluminide Coating of Iron

R. W. Heckel,* M. Yamada,** C. Ouchi,** and A. J. Hickl***

Abstract

The kinetics of phase layer growth during the aluminization of Fe and during subsequent heat treatment (homogenization) were investigated. Pack processing was employed for aluminization; the variables studied were temperature, time, amount of Al powder in the pack, and the Al powder particle size. Homogenization was studied as a function of temperature, time, and extent of prior aluminization treatment. A predictive model was developed to describe the changes in coating microstructure as a function of processing parameters.



*Department of Metallurgical Engineering, Michigan Technological University, Houghton, Michigan

**Nippon Kokan K. K., Technical Research Center, Kawasaki, Japan

***Stellite Division, Cabot Corporation, Kokomo, Indiana

(Research performed at Carnegie-Mellon University, Pittsburgh, PA)

Introduction

Aluminization of iron and iron-base alloys is of importance in the protection of these materials from high-temperature oxidation and corrosion, including sulfur bearing environments (1-5). Substrates for aluminization have ranged from plain carbon steel to stainless steel. Although a variety of processes can be used to diffuse Al into the surface of steel, the most readily adapted method is to place the article to be diffusion coated into a pack containing powdered Al (or an Al alloy), an activator such as NH_4Cl , and Al_2O_3 (which disperses the Al and activator and remains inert during the aluminization). At elevated temperatures, the activator reacts with the Al and provides for gas-phase transport through the pack to the surface of the steel. The details of the pack process have been studied extensively (6-8).

Heat treatment of aluminized coatings can provide an additional degree of control over the microstructure of the coating. Thus, aluminization by the pack process can be used as a rapid method for increasing the Al content of the near surface region; subsequent homogenization heat treatment in an inert environment can be employed to adjust the coating microstructure to provide the optimum phase layer thicknesses and to select the specific surface phase necessary for the intended application. If Al neither enters or leaves the surface during the homogenization treatment, the mass of Al in the material remains constant during this process. Homogenization treatment of aluminide coatings on Ni has already been studied (9).

The aluminization and homogenization processes are represented schematically in terms of Al concentration-distance profiles in Figure 1. The formation of the η (FeAl_2) and ζ (Fe_2Al_5) phase layers were shown in the present study to form on the surface of the Fe during aluminization. The η phase has a range of compositions* from $C_{\eta\zeta} = 0.70$ to $C_{\eta\theta} = 0.72$; the ζ phase

*All compositions will be referred to as atomic fractions.

ranges in composition from $C_{\zeta\eta} = 0.67$ to $C_{\zeta\alpha} = 0.65$ (10). The α phase referred to in Figure 1 ranges from $C_{\alpha\zeta} = 0.52$ to zero (pure Fe) and therefore denotes the Al-enriched α solid solution of Fe.* The aluminization process proceeds by movement of the η/ζ and ζ/α interfaces into the Fe and thickening of the α layer. Since the mass of the system increases, the surface of the material must also move outward. The linear concentration gradient approximation shown in Figure 1 facilitates the determination of the amount of Al added to the system from a knowledge of the phase layer thicknesses, x_i 's:

$$M = x_{\eta} \left(\frac{C_{\eta\theta} + C_{\eta\zeta}}{2} \right) + x_{\zeta} \left(\frac{C_{\zeta\eta} + C_{\zeta\alpha}}{2} \right) + x_{\alpha} \left(\frac{C_{\alpha\zeta}}{2} \right) \quad (1)$$

M has units of length and increases with time during the aluminization process.

Aluminization and/or homogenization above 910°C will also result in the formation of the γ phase in the Fe substrate. However, the low solubility of Al in the γ phase and the low interdiffusion coefficient in this phase resulted in a negligible effect on the kinetics measured in the present investigation. Thus, no further consideration will be given to γ -phase formation in this paper.

The homogenization process as shown in Figure 1 proceeds in three sequential stages all of which can be characterized by a constant value of M resulting from the prior aluminization treatment. Since the flux of Al into the surface is zero during homogenization (i.e., $M = \text{constant}$), the η phase decreases in thickness during Stage I as the ζ and α increase in thickness. Stage II begins when $x_{\eta} = 0$ and proceeds with decreasing x_{ζ} and increasing x_{α} . Stage III begins when $x_{\zeta} = 0$ and proceeds with increasing x_{α} and decreasing surface concentration of Al. Thus, proper control of the homogenization process allows for the selection of (a) the most suitable surface phase (η , ζ , or α) for the intended application, (b) the optimum phase layer thicknesses, and

*The composition range up to 0.52 includes the β_2 ordered solid solution as well as the random solid solution (10).

(c) the optimum surface concentration of Al.

Studies on the aluminization and subsequent homogenization of phase layers on Ni have shown that phase layer growth is controlled by long range lattice diffusion through the phase layers (9). Since this parabolic behavior should also apply to Fe substrates, phase layer growth rates should be proportional to the reciprocal of the layer thickness:

$$\frac{dx_i}{dt} = \frac{K_i}{x_i} \quad (2)$$

where x_i is the thickness of the i^{th} phase and K_i is the parabolic rate constant for the growth of the i^{th} phase. For aluminization, Eq. (2) integrates to:

$$x_i^2 = 2 K_i t \quad (3)$$

For homogenization, Eq. (2) integrates to

$$x_i^2 - x_{i0}^2 = 2 K_i (t - t_0) \quad (4)$$

where x_{i0} is the initial thickness of the i^{th} phase and t_0 is the homogenization time at the beginning of the homogenization stage of interest. For example, for Stage I, $x_{\zeta 0}$ is the thickness of the ζ phase after aluminization and $t_0 = 0$. The foregoing analysis applies only to those phases which grow during homogenization; the decrease in x_{η} and x_{ζ} during Stages I and II, respectively, should not proceed parabolically, since, except for a short initial transient period, diffusion should not take place in these phases as they decrease in thickness.

The purpose of the present investigation was threefold:

- a. to provide additional understanding of the process of aluminide coating of Fe,
- b. to measure the kinetics of phase growth during aluminization and homogenization,

c. to formulate a predictive model capable of defining the effects of processing variables on coating microstructure.

Experimental Procedure

Ferrovac E Fe was used as the substrate material in this study; impurities were all less than 60 weight ppm except for Ni (210) and Cr (100). Aluminization of Fe specimens was carried out in 30 to 50 cm³ covered Fe crucibles. The pack contained 3 weight percent NH₄Cl as an activator; the Al powder in the pack was varied from 10 to 35 weight percent and three mesh sizes were studied (-20, -100, and -325). Homogenization treatments were carried out in an argon atmosphere. Coating microstructures were studied by light microscopy to obtain layer thicknesses,* x-ray diffraction to identify phases, and electron microprobe techniques to identify phases and to obtain concentration distance profiles (11).

Experimental Results

Typical thickening data for the η , ζ , and α phases during aluminization are presented in Figure 2. No evidence of the θ (FeAl₃) phase was found and no significant incubation period was observed. Thus, all data were found to conform with Eq. (3). The thickening of the ζ and α phases was found to be independent of pack conditions; the η phase growth rate increased with increasing Al concentration in the pack and decreasing Al powder particle size. The η phase growth rate appeared to reach a maximum at about 35 percent Al and -100 mesh powder; presumably, these conditions resulted in a saturated η -phase composition ($C_{\eta\theta}$) at the surface of the specimen. The parabolic rate constants for the aluminization study (slopes of lines in Figure 2) are given in Table I.

Typical thickening data for the ζ and α phases during homogenization are

*An average of 40 to 80 measurements for each determination.

TABLE I

Experimentally determined parabolic rate constants (from $X^2 = 2Kt$) for aluminization.

Temperature (°C)	Pack Conditions		K_1	$K_1 \text{ } ((\mu\text{m})^2/\text{sec})$	
	Weight Percent Al	Al Mesh Size		K_η	K_ζ
780	35	-100	1.4	*	0.0045
830	10	-100	0.71	0.000088	0.012
830	15	-20	0.64	0.000088	0.0094
830	15	-100	1.5	0.000088	0.012
830	15	-325	1.5	0.000088	0.0094
830	25	-100	2.2	0.000088	0.012
830	35	-100	2.5	0.000088	0.012
880	35	-100	5.0	0.00080	0.043
925	35	-100	7.7	0.0050	0.10
1000	35	-100	10.7	0.062	0.59

* ζ layer too thin to be measured

presented in Figure 3. The growth is parabolic, in accord with Eq. (4), with no significant incubation period; the transition in boundary conditions from aluminization to homogenization thus appears to take place rapidly. The parabolic rate constant data for homogenization (slopes of lines in Figure 3) are given in Table II. The relative insensitivity of K_α to the stage of homogenization indicates that the value obtained during Stage I may be used in Stages II and III.

Concentration-distance profiles obtained by electron microprobe analysis of specimens given homogenization treatments (all three stages) are presented in Figure 4. These curves are seen to be in general agreement with the schematic curves presented in Figure 1. However, it is significant that the α -phase profiles are not linear, and, in fact show evidence of a variation in the interdiffusion coefficient with composition in both the β_2 phase (concentrations greater than 0.25) and random solid solution α phase (concentrations less than 0.25) which is consistent with published data (12).

Discussion

A predictive model for describing the growth and shrinkage rates of the η , ζ , and α phases during aluminization and homogenization can be formulated from the data of the present study (Tables I and II) combined with Equations 1, 3, and 4. Equations 3 and 4 define the thicknesses of growing phases directly; Eq. (1) may be used to obtain the thicknesses of the shrinking phases. Furthermore, the changing surface concentration during Stage III may be approximated as:

$$C_s \approx \frac{2M}{X_\alpha} \quad (5)$$

where C_s is the surface concentration in Stage III, by equating M to the area under the linear gradient (Figure 1).

TABLE II

Experimentally determined parabolic rate constants (from $X^2 - X_0^2 = 2K(t - t_0)$) for homogenization.

Temperature (°C)	Homogenization Stage	$\frac{K_1}{K_\zeta} ((\mu\text{m})^2/\text{sec})$	$\frac{K_1}{K_\alpha}$
780	I	0.0050	0.019
830	I	0.022	0.061
895	I	0.055	0.23
925	I	0.11	0.37
950	I	0.16	0.53
1000	I	0.38	1.6
950	II		0.66*
950	III		0.57*

*Aluminized at 830°C for 3.6×10^3 sec with 15 w/o -100 mesh Al in pack, giving $M = 8 \times 10^{-5}$ m. Data valid for Stage II ($1.2 \times 10^4 < t < 2.9 \times 10^4$ sec) and for Stage III up to 9.4×10^4 sec.

The critical experiment to test this model was performed by homogenizing three sets of samples given different aluminizing treatments (780°C, 1700 sec, 35 w/o -100 mesh Al; 830°C, 3100 sec, 10 w/o -100 mesh Al; 830°C, 3500 sec, 15 w/o -20 mesh Al), but all having $M = 5 \times 10^{-5}$ m. A comparison of the model predictions (solid lines) and the three sets of homogenization data are presented in Figure 5. Clearly, variations between the homogenization behavior of the three sets of data are negligible, thus validating the use of the M parameter to describe the initial condition for homogenization. Furthermore, the experimental data agree with the model predictions for both the thicknesses of the phase layers and the times for the transitions between the homogenization stages. However, it should be noted that the experimentally determined surface concentration during Stage III is somewhat less than the model prediction (Eq. (5)). The reason for this discrepancy arises from the fact that the actual surface concentration is less than what would be predicted from a linear gradient (see probe data in Figure 4).

Conclusions

The effects of processing parameters on the microstructure of aluminide coatings on pure Fe can be reliably predicted from a knowledge of parabolic growth rate constants. The key to this modeling procedure is to define the initial condition for homogenization in terms of the total amount of Al entering the system as a result of aluminization, M . The value of M may be readily obtained from the phase layer thicknesses or from electron microprobe data. The procedures employed in the present investigation should be applicable to the diffusion coating of other substrate materials.

Acknowledgments

The authors are grateful for the support of the Metallurgy Branch of the

Office of Naval Research in this research. In addition, the authors acknowledge many fruitful discussions with H. C. Bhedwar during the course of the research and the preparation of the manuscript.

References

1. S. L. Case, Steel Processing, 1950, p. 435.
2. J. H. Nicholls, Metallurgia, vol. 75, 1967, p. 57.
3. Metals Handbook, vol. 2, American Society for Metals, 1964, p. 489.
4. P. G. Gabe, ISI IDM Meeting on Physical Metallurgy Aspects of Surface Coatings, London, May 1973, p. 127.
5. W. A. McGill and M. J. Weinbaum, Metal Protection and Performance, July 1972, p. 28.
6. G. W. Goward, D. H. Boone and C. S. Giggins, Transactions Quarterly ASM, vol. 60, 1967, p. 228.
7. S. R. Levine and R. M. Caves, Journal of Electrochemical Society, vol. 121, 1974, p. 1051.
8. R. Sivakumar and L. L. Seigle, Metallurgical Transactions, vol. 7A, 1976, p. 1073.
9. A. J. Hickl and R. W. Heckel, Metallurgical Transactions, vol. 6A, 1975, p. 431.
10. M. Hansen, Constitution of Binary Alloys, McGraw-Hill, 1958, p. 90.
11. D. Laguitton, R. Rousseau and F. Claise, Analytical Chemistry, vol. 47, 1975, p. 2174.
12. K. Hirano and A. Hishinuma, Transactions of Japan Institute of Metals, vol. 32, 1968, p. 516.

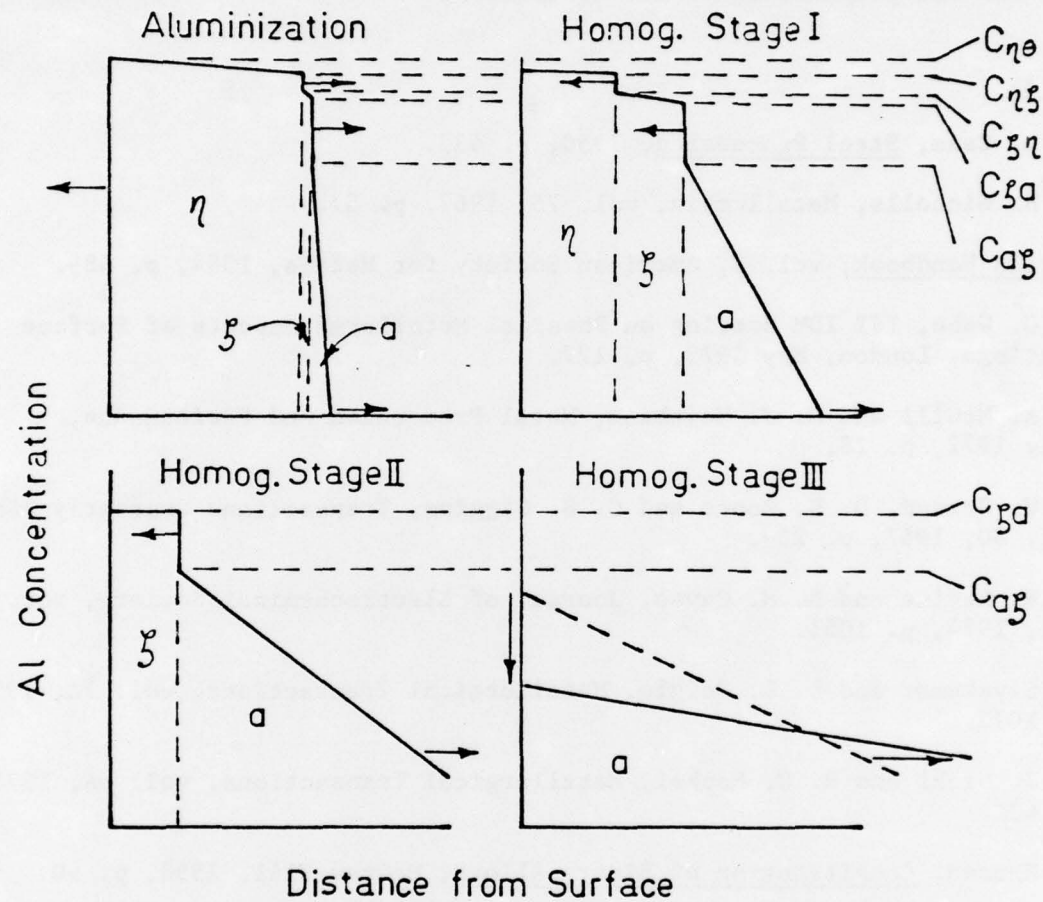


Figure 1. Schematic representation of concentration-distance profiles during aluminization and homogenization.

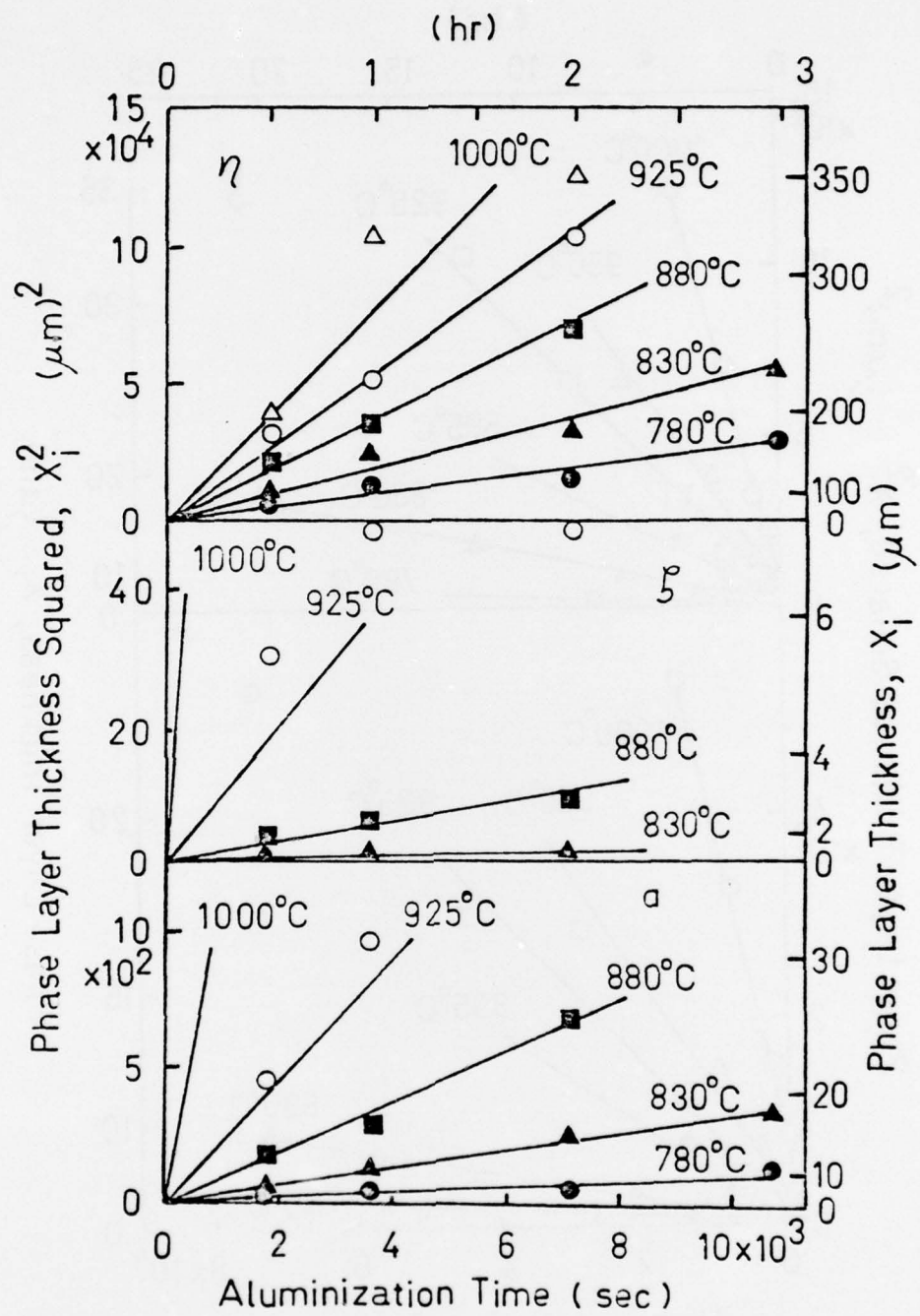


Figure 2. Growth data for the η , ζ , and α phase layers during aluminization of Fe. The pack contained 35 weight percent of -100 mesh Al powder.

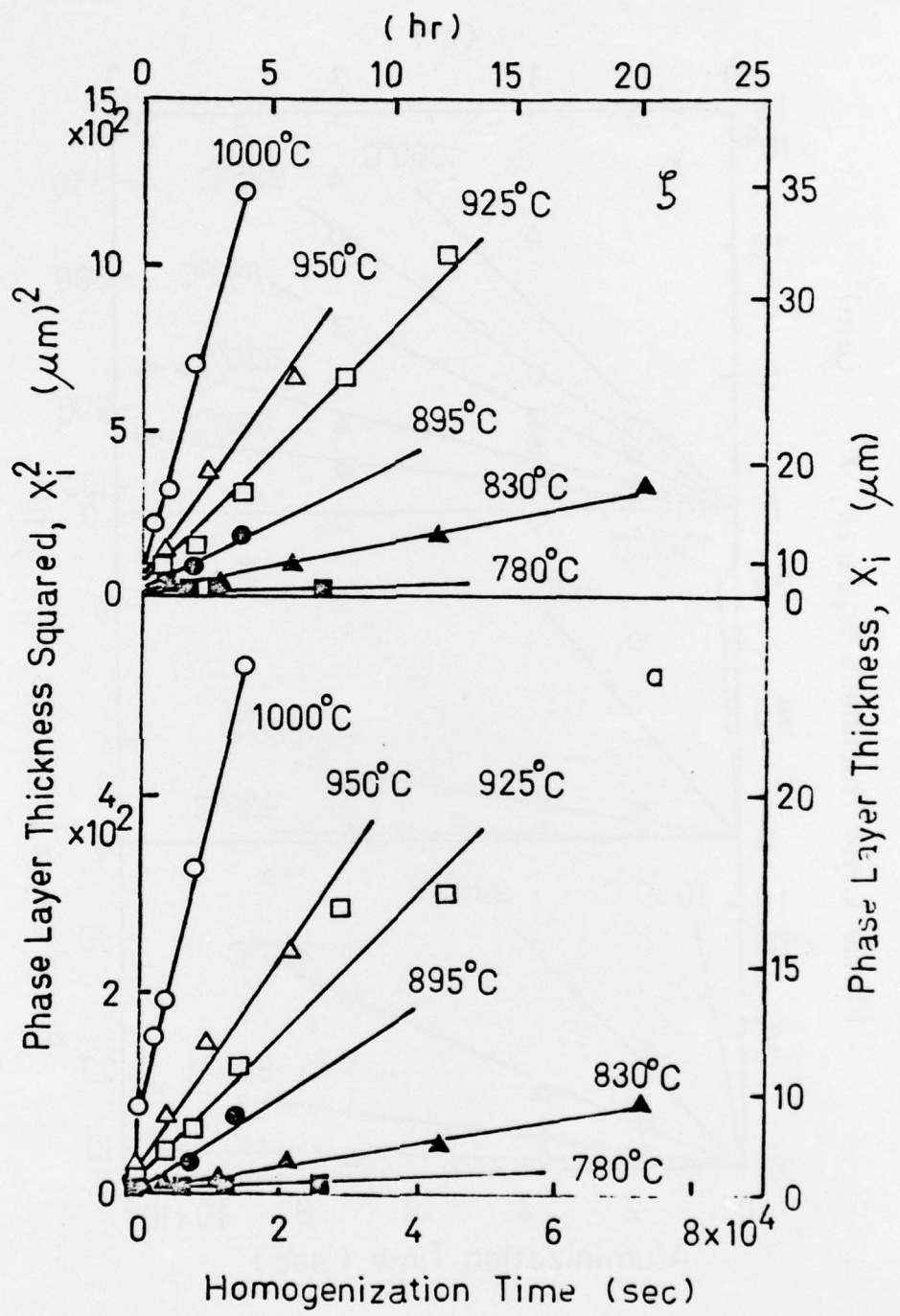


Figure 3. Growth data for the ζ and α phase layers during the Stage I homogenization process.

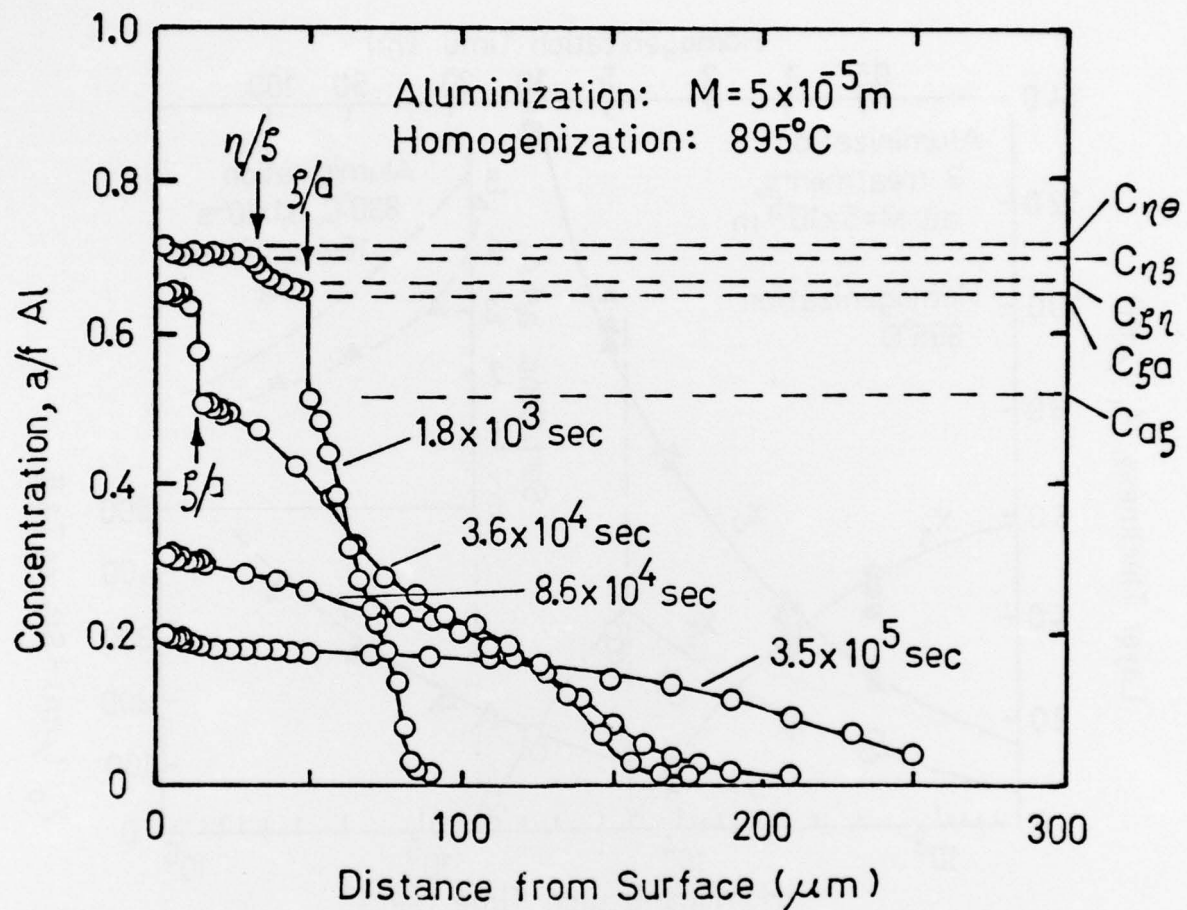


Figure 4. Electron microprobe data for four concentration-distance profiles during the homogenization of specimens previously aluminized to $M = 5 \times 10^{-5} \text{ m}$. One curve shown for Stage I, one for Stage II, and two for Stage III.

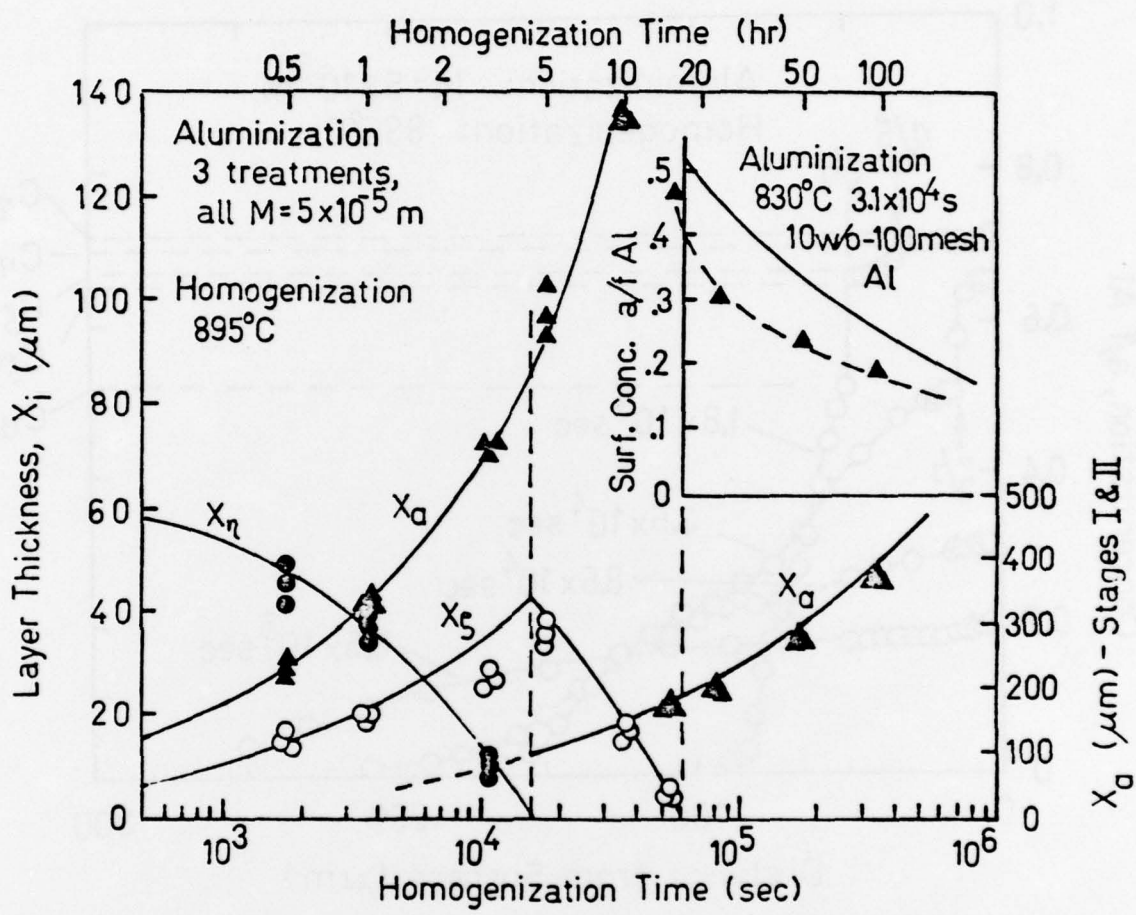


Figure 5. Comparison of model predictions and experimental data for homogenization for three different aluminization treatments all having $M = 5 \times 10^{-5} \text{ m}$.

Unclassified

SECURITY CLASSIFICATION OF THIS PAGE (When Data Entered)